IOP Conf. Series: Materials Science and Engineering **225** (2017) 012100 doi:10.1088/1757-899X/225/1/012100

A Theoretical Model for Estimation of Yield Strength of Fiber Metal Laminate

Sunil Bhat[a], Suresh Nagesh[b], C K Umesh[c] and S Narayanan[d]
[a,b]Professor, PES University, Bangalore-560087, Karnataka, India
[d] Senior Professor, VIT University, Vellore-632014,Tamil Nadu, India

Abstract: The paper presents a theoretical model for estimation of yield strength of fiber metal laminate. Principles of elasticity and formulation of residual stress are employed to determine the stress state in metal layer of the laminate that is found to be higher than the stress applied over the laminate resulting in reduced yield strength of the laminate in comparison with that of the metal layer. The model is tested over 4A-3/2 Glare laminate comprising three thin aerospace 2014-T6 aluminum alloy layers alternately bonded adhesively with two prepregs, each prepreg built up of three uni-directional glass fiber layers laid in longitudinal and transverse directions. Laminates with prepregs of E-Glass and S-Glass fibers are investigated separately under uni-axial tension. Yield strengths of both the Glare variants are found to be less than that of aluminum alloy with use of S-Glass fiber resulting in higher laminate yield strength than with the use of E-Glass fiber. Results from finite element analysis and tensile tests conducted over the laminates substantiate the theoretical model.

Keywords: E-Glass fiber, Fiber metal laminate, Glare, S-Glass fiber, Yield strength

1. INTRODUCTION

Fiber metal laminate (FML) is a hybrid material system that is constructed with layers of thin and light metallic sheets which are alternately bonded adhesively with composite prepregs by heat and pressure, each prepreg built up of fiber layers laid in similar or different orientations. FML exhibits excellent fatigue and fracture resistance due to bridging or diversion of load from soft cracked metallic layers towards ultra-strong fibers in prepregs thus making the laminate a better substitute, even at increased cost, for monolithic metals and their alloys in aerospace applications where fatigue and fracture properties assume importance. As the result, research work on FML's has so far been mostly directed at their fatigue and fracture aspects. However results, albeit limited, are also available on strength properties of FML's. In experimental field, Lawcock *et al.* [1] studied the effect of adhesive bonding between aluminum alloy sheets and carbon fiber based composite prepregs on strength of the laminate. Kawai *et al.* [2] presented off-axis strength behaviour of glass fiber and aluminum alloy based FML (Glare). Cortes and Cantwell [3] measured tensile properties of laminates constructed with carbon fiber reinforced PEEK and titanium layers. Khalili *et al.* [4] tested FML samples from various lay ups of glass fiber/epoxy resin with steel and aluminum alloy layers and compared their strengths with each other and with monolithic metals and conventional fiber-resin composites (FRP's). Torshizi *et*

al. [5] examined tensile properties of Glare and kevlar fiber based FML (Arall). Sinmazcelik *et al.* [6] investigated surface treatment procedures of metals and their bonding techniques with composites that was followed by measurement of tensile strengths of different types of FML's. In numerical field, Rooijen *et al.* [7] developed a finite element model for understanding the bearing behaviour of Glare. The plasticity in metal layers, failure of fiber layers and frictional effects between the layers were incorporated in the model. Krimbalis *et al.* [8] presented finite element model for estimation of compressive characteristic dimension (CCD) in various Glare variants. A novel re-definition of conventional CCD governed by yield strength of aluminum alloy was proposed. In theoretical field, Schuerch [9] developed a model with the help of plasticity characteristics to predict uni-axial ultimate compressive strength and failure modes of unidirectional composites. The model was extended to boron fiber and magnesium metal matrix composite that resembled the configuration of a FML. Literature review reveals a limited theoretical work being reported on FML's. As such, there exists the need for theoretical models to assess the mechanical properties of the laminates. Determination of properties in absence of theoretical models calls for extensive numerical analysis or fabrication of large number of test specimens for accumulation of reliable data. Moreover, a theoretical model always proves to be handy in design stage of any structure.

The magnitude of stress that develops or is induced in each metal layer of a FML differs from the stress applied over the laminate in service conditions due to i) Redistribution of stress in dissimilar and elastically un-identical material layers of the laminate to fulfil the requirement of equal strain in all the layers necessitated by the principles of structural mechanics and ii) Inherent presence of variable residual stresses in material layers that are generated during high temperature curing of the laminate due to different coefficients of thermal expansion of the materials. Based on these facts, a theoretical model is presented with the help of the principles of elasticity and formulation of residual stress to obtain the induced stress in metal layer, the magnitude of which is found to be higher than that of applied stress that implies reduced yield strength of the laminate vis-à-vis the metal layer (Yield strength refers to uni-axial value). The model is tested over 4A-3/2 Glare laminate comprising 2014-T6 aerospace aluminum alloy layers and uni-directional glass fiber based prepregs. Laminates with prepregs of E-Glass and S-Glass fibers are investigated separately under uni-axial tension. Yield strengths of both the Glare variants are confirmed to be less than that of aluminum alloy with use of S-Glass fiber resulting in higher laminate yield strength than with the use of E-Glass fiber. The laminates are modelled by finite element method and are fabricated for numerical assessment and experimental measurement of their yield strengths respectively. Theoretical model is validated by finite element and experimental results.

2. THEORETICAL MODEL

Refer Fig. 1 that illustrates the stacking sequence of material layers in a FML. Elastic stress-strain, $\sigma - \varepsilon$, constitutive equations of constituent materials in two dimensional (*x*-*y*) plane are conventionally expressed as $\begin{Bmatrix} \sigma_x \\ \sigma_y \\ \tau_{xy} \end{Bmatrix} = \{M\} \begin{Bmatrix} \varepsilon_x \\ \varepsilon_y \\ \gamma_{xy} \end{Bmatrix}$ where σ and τ are normal and shear stresses whereas ε and γ are normal and shear strains respectively. Since the material layers in

the laminate are thin, plane stress condition is adopted i.e. $\sigma_z = 0$. Stiffness matrices of materials, $\{M\}$, in such a condition are expressed in terms of their elastic parameters as $\begin{bmatrix} \frac{E_x}{1-\upsilon^2} & \frac{\upsilon E_x}{1-\upsilon^2} & 0 \\ \frac{\upsilon E_y}{1-\upsilon^2} & \frac{E_y}{1-\upsilon^2} & 0 \\ 0 & 0 & \mu_{xy} \end{bmatrix}$ where E, μ and υ represent the modulus of elasticity, shear modulus and poisson's ratio of the material layer respectively. $E_x = E_y$ for isotropic metal, *m*, and resin, *r*, layers respectively. $E_x \neq E_y$ if fiber, *f*, is unisotropic like carbon, kevlar etc. Since the laminate, *lam*, under tension in service condition is considered to yield and therefore fail when its soft metal layers yield with prepregs remaining intact due to the presence of ultra-strong fibers in them, attention is focused on elastic stress state in metal layers whose magnitude is decided by overall stiffness of the laminate. Generalized form of elastic stiffness matrix of the laminate, $\{M\}_{lam}$, with strong adhesive bond between dissimilar metal and fiber layers and which contains, *n*, number of

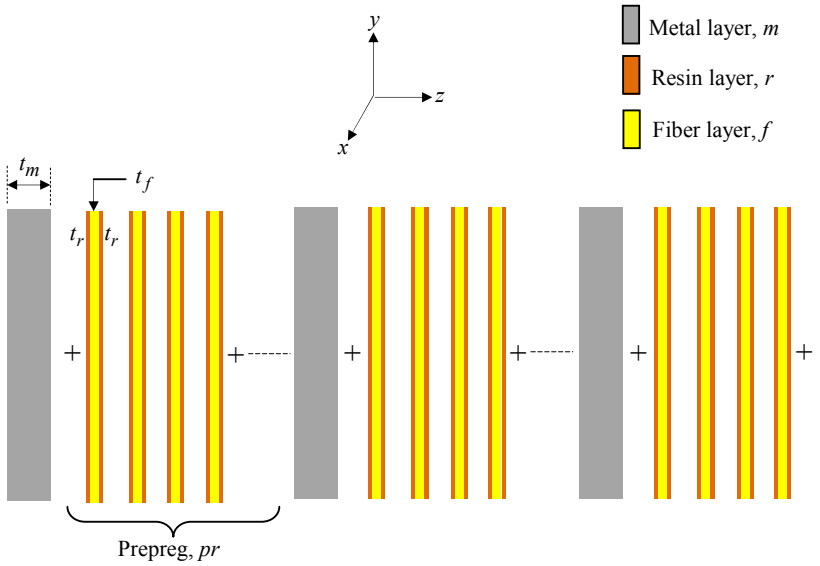

Fig. 1. Stacking sequence in fiber metal laminate

material layers of thickness, *t*, is written from classical theory as the sum of the stiffness of the ingredients in the form

$$\{M\}_{lam} = \{M\}_m \times \frac{t_m \times n_m}{t_{lam}} + \{M\}_{f0} \times \frac{t_{f0} \times n_{f0}}{t_{lam}} + \{M\}_{f90} \times \frac{t_{f90} \times n_{f90}}{t_{lam}} + \{M\}_r \times \frac{t_r \times n_r}{t_{lam}} \quad (1)$$

where t_{lam} is the thickness of the laminate and f_0 and f_{90} represent uni-directional fiber layers laid in *y* and *x* directions respectively. In case the fiber layers are oriented at an angle in *x*-*y* plane or if bi-directional fiber layers are used, stiffness matrix, $\{M\}$, of fibers used in Eq. (1) shall only change with expression of $\{M\}_{lam}$ remaining the same. Residual strains and stresses in the

material layers are assumed to be uniform in order to evolve a workable model. Residual strain, $\{\varepsilon\}_{rs,m}$, in the metal layer is obtained from

$$\{\varepsilon\}_{rs,m} = \left[\begin{Bmatrix} \alpha_x \\ \alpha_y \\ 0 \end{Bmatrix}_m - \begin{Bmatrix} \alpha_x \\ \alpha_y \\ 0 \end{Bmatrix}_{lam} \right] \times \left(T_{curing} - T_{ambient} \right) \tag{2}$$

where α is coefficient of thermal expansion and T_{curing} and $T_{ambient}$ are laminate curing and ambient temperatures. Residual strain in *z* direction is neglected due to small thickness of the layer. Strain developing in metal layer upon application of tensile stress, $\sigma_{applied}$, over the laminate in service conditions is equal in all the material layers and is written as $\{\varepsilon\}_{applied,m} = \{\varepsilon\}_{lam} = \{M\}_{lam}^{-1} \sigma_{applied}$. Total strain in metal layer is found by superimposing residual and applied strains as, $\{\varepsilon\}_{induced,m} = \{\varepsilon\}_{rs,m} + \{\varepsilon\}_{appied,m}$, following which the induced stress developing in each metal layer is determined from

$$\{\sigma\}_{induced,m} = \{M\}_m \times \{\varepsilon\}_{induced,m} = \{M\}_m \times \left[\{\varepsilon\}_{rs,m} + \{\varepsilon\}_{applied,m} \right] \tag{3}$$

where terms $\{M\}_m \times \{\varepsilon\}_{rs,m}$ and $\{M\}_m \times \{\varepsilon\}_{applied,m}$ denote residual and redistributed stresses in the layer respectively. For the laminate subjected to uni-axial tension in *y* direction i.e. $\sigma_{applied} = \begin{Bmatrix} 0 \\ \sigma_y \\ 0 \end{Bmatrix}_{applied}$, the expression for induced stress in the metal layer assumes the following form

$$\begin{Bmatrix} \sigma_x \\ \sigma_y \\ \tau_{xy} \end{Bmatrix}_{induced,m} = \{M\}_m \left\{ \left[\begin{Bmatrix} \alpha_x \\ \alpha_y \\ 0 \end{Bmatrix}_m - \begin{Bmatrix} \alpha_x \\ \alpha_y \\ 0 \end{Bmatrix}_{lam} \right] \times \left(T_{curing} - T_{ambient} \right) + \{M\}_{lam}^{-1} \times \begin{Bmatrix} 0 \\ \sigma_y \\ 0 \end{Bmatrix}_{applied} \right\} \tag{4}$$

Eq. (4) indicates induced stress in metal layer to be higher than the applied stress. Since the possibility of buckling and separation of material layers of the laminate are minimal in case of tensile loading, design stress in metal layer that is the function of induced stress is justifiably presumed to be equal to yield strength of metal at the juncture when the laminate yields. Corresponding stress applied over the laminate represents the uni-axial yield strength, $\{YS\}_{lam}$, of the laminate. Application of Eq. (4) at yield or critical condition (*) of the laminate results in

$$\begin{Bmatrix} \sigma_x \\ \sigma_y \\ \tau_{xy} \end{Bmatrix}_{induced,m*} = \{M\}_m \left\{ \left[\begin{Bmatrix} \alpha_x \\ \alpha_y \\ 0 \end{Bmatrix}_m - \begin{Bmatrix} \alpha_x \\ \alpha_y \\ 0 \end{Bmatrix}_{lam} \right] \times \left(T_{curing} - T_{ambient} \right) + \{M\}_{lam}^{-1} \times \begin{Bmatrix} 0 \\ YS \\ 0 \end{Bmatrix}_{lam} \right\} \tag{5}$$

Eq. (5) is rearranged to determine $\{YS\}_{lam}$ as follows

$$\{M\}_m \times \{M\}_{lam}^{-1} \times \begin{Bmatrix} 0 \\ YS \\ 0 \end{Bmatrix}_{lam} = \begin{Bmatrix} \sigma_x \\ \sigma_y \\ \tau_{xy} \end{Bmatrix}_{induced,m*} - \{M\}_m \left\{ \left[\begin{Bmatrix} \alpha_x \\ \alpha_y \\ 0 \end{Bmatrix}_m - \begin{Bmatrix} \alpha_x \\ \alpha_y \\ 0 \end{Bmatrix}_{lam} \right] \times \left(T_{curing} - T_{ambient} \right) \right\} \tag{6}$$

2.1 Solution

A numerical iterative procedure is adopted to solve Eq. (6). Suitable value of $\{YS\}_{lam}$ is assumed at LHS in each iteration to determine the unknown induced stress state in metal layer in x and y directions at RHS with shear stress component equal to zero. Using distortional energy theory as yield criterion of ductile metal layer, the magnitude of von-Mises stress, in case of principal stress state existing in x-y plane of the layer, given by $\left[\sqrt{\frac{\left(\sigma_{y,induced,m}-\sigma_{x,induced,m}\right)^2+\left(\sigma_{y,induced,m}\right)^2+\left(\sigma_{x,induced,m}\right)^2}{2}}\right]$, is obtained in every iteration. $\{YS\}_{lam}$ is changed till von-Mises stress in metal layer is equal to known value of yield strength of metal. The value of $\{YS\}_{lam}$ when the above condition is satisfied represents uni-axial yield strength of the laminate. Since the critical value of induced stress state in the metal layer i.e. at the instant of yielding is the measure of yield strength of the laminate, Eq. (6) clearly predicts the yield strength of the laminate to be lesser than that of the metal layer.

3. RESULTS AND DISCUSSION

Refer Fig. 2. The theoretical model is tested over Glare laminate comprising three thin, 0.4 mm, 2014-T6 aerospace aluminum alloy layers, *al*, alternately bonded with two glass fiber based composite prepregs at curing temperature of 160 deg. C under pressure of 10 bar. Each prepreg is built up of three composite layers, *c*0, *c*90 and *c*0 in sequence where *c*0 and *c*90 denote epoxy resin and CY205 (Hardener) impregnated f_0 and f_{90} uni-directional fibers respectively. The fiber layer is of plain weave type with grammage of 110 gsm and thickness of 0.1 mm. The grade of Glare with chosen configuration is 4A-3/2 (4A denotes 0-90-0 orientation of composites in prepreg and 3/2 indicates the number of aluminum alloy layers and prepregs in the laminate). Laminates with E-Glass and S-Glass fibers, both the fibers being isotropic in nature, are investigated separately under uni-axial tension. Material properties are presented in Table 1. Dimensional data of the laminate are $n_{al} = 3$, $n_{f0} = 4$,

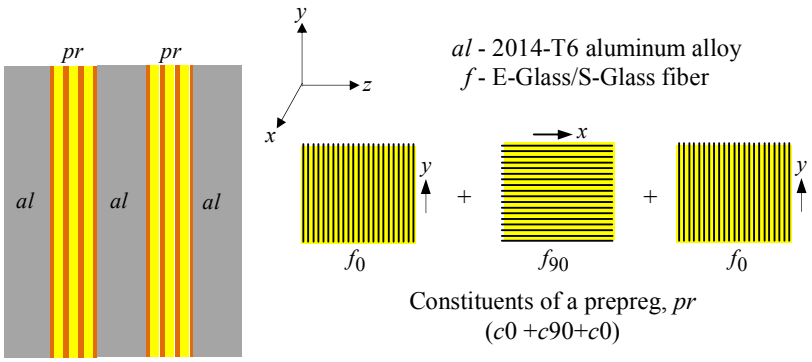

Fig. 2. Construction of investigated Glare (Cross sectional view)

$n_{f90} = 2$, $n_r = 12$, $t_{al} = 0.4$ mm, $t_{f0} = t_{f90} = 0.1$ mm and $t_r = 0.0455$ mm. Volume fractions are $v'_f = 0.522, v'_r = 0.478$, $v'_{al} = 0.51$, $v'_{c0} = 0.32$ and $v'_{c90} = 0.17$. The laminate is 200 mm long (y direction), 50 mm wide (x direction) with expected thickness, t_{lam}, (z direction) of 2.346 mm that is estimated from ($n_{al}t_{al} + n_{f0}t_{f0} + n_{f90}t_{f90} + n_r t_r$).

Table 1. Material properties

	Al. 2014- T6 alloy, *al*	Fiber, *f* E-Glass	Fiber, *f* S-Glass	Epoxy resin, *r*
Modulus of elasticity, *E* (MPa)	72000	71000	85500	3500
Shear modulus, μ (MPa)	27060	29700	35000	1250
Poisson's ratio, υ	0.33	0.22	0.22	0.33
Yield strength (MPa)	372	-	-	-
Ultimate tensile strength (MPa)	415	3450	3450	60
Percent elongation	8.0	4.8	4.0	4.0
Coeff. of thermal expansion, α (C^{-1})	23×10^{-6}	5×10^{-6}	5×10^{-6}	57.5×10^{-6}

Eq. (6) when applied at yield state of Glare that uses aluminum alloy as metal changes to

$$\{M\}_{al} \times \{M\}_{Glare}^{-1} \times \begin{Bmatrix} 0 \\ YS \\ 0 \end{Bmatrix}_{Glare} = \begin{Bmatrix} \sigma_x \\ \sigma_y \\ \tau_{xy} \end{Bmatrix}_{induced,al*} - \{M\}_{al} \left\{ \left[\begin{Bmatrix} \alpha_x \\ \alpha_y \\ 0 \end{Bmatrix}_{al} - \begin{Bmatrix} \alpha_x \\ \alpha_y \\ 0 \end{Bmatrix}_{Glare} \right] \times \left(T_{curing} - T_{ambient} \right) \right\} \quad (7)$$

Refer Appendix A for stiffness matrices that are obtained with the help of previously stated formulations. Refer Appendix B for fundamental equations of composites/laminates that lead to the evaluation of the coefficients of thermal expansion of Glare as $\begin{Bmatrix} \alpha_x \\ \alpha_y \\ 0 \end{Bmatrix}_{Glare} = \begin{Bmatrix} 19.77\times10^{-6} \\ 19.40\times10^{-6} \\ 0 \end{Bmatrix}$ with use of E-Glass fiber and $\begin{Bmatrix} \alpha_x \\ \alpha_y \\ 0 \end{Bmatrix}_{Glare} = \begin{Bmatrix} 20.18\times10^{-6} \\ 18.80\times10^{-6} \\ 0 \end{Bmatrix}$ with use of S-Glass fiber. On substituting T_{curing} as 160 deg. C, $T_{ambient}$ as 30 deg. C and other requisite parameters in Eq. (7), the values of $\begin{Bmatrix} 0 \\ YS \\ 0 \end{Bmatrix}_{Glare}$ with use of E-Glass and S-Glass fibers are obtained as $\begin{Bmatrix} 0 \\ 270 \\ 0 \end{Bmatrix}$ MPa and $\begin{Bmatrix} 0 \\ 282 \\ 0 \end{Bmatrix}$ MPa respectively while corresponding critical stress values in aluminum alloy layer i.e. $\begin{Bmatrix} \sigma_x \\ \sigma_y \\ \tau_{xy} \end{Bmatrix}_{induced,al*}$ are equal to $\begin{Bmatrix} 60.71 \\ 399.73 \\ 0 \end{Bmatrix}$ MPa and $\begin{Bmatrix} 55.1 \\ 397.5 \\ 0 \end{Bmatrix}$ MPa in former and in latter case. As is

evident from the results, uni-axial yield strengths of both the Glare variants, determined as 270 MPa and 282 MPa, are less than 372 MPa i.e. the uni-axial yield strength of aluminum alloy. Also, S-Glass fiber is found to result in increased yield strength of Glare because of its higher modulus of elasticity than that of E-Glass fiber.

4. MODEL VALIDATION

The theoretical model is validated with the help of finite element analysis and experimental work that are discussed as follows:-

4.1 Finite element analysis

Refer Fig. 3. 3D finite element models of investigated Glare with prepregs of E-Glass and S-Glass fibers were constructed separately in Ansys software. Solid 185 elements were used to discretize aluminum alloy layers. Since solid elements tend to lock in thin applications, shell 190 elements were chosen to mesh thin fiber and resin layers. Known elastic-plastic stress strain data of aluminum alloy, linear elastic data of fiber and non-linear elastic data of resin were substituted in the material models. Uniform residual stresses in *x* and *y* directions in aluminum alloy, fiber and resin layers, obtained theoretically from the expressions, $\{M\}_{al} \times \{\varepsilon\}_{rs,al}$, $\{M\}_{f} \times \{\varepsilon\}_{rs,f}$ and $\{M\}_{r} \times \{\varepsilon\}_{rs,r}$ respectively, as explained in Section 2, were externally introduced as initial stress at all respective nodes in material layers with the help of a pre-processor code. The residual stresses were different in laminates with E-Glass and S-Glass fibers. Their magnitudes are presented in Table 2. The nodes at material interfaces were merged and their connectivity was checked. The model was constrained in all degrees of freedom at one end whereas tensile stress, $\sigma_{y,applied}$, was applied at the other end (in *y* direction) to simulate uni-axial tension. The magnitude of $\sigma_{y,applied}$ was increased till the value of von-Mises stress in aluminum alloy layers reached 372 MPa i.e. the yield strength of aluminum alloy.

Refer Fig. 4 for von-Mises stress plots in external aluminum alloy layer of the laminate at different values of $\sigma_{y,applied}$. The layers displayed yielding all across their width at $\sigma_{y,applied}$ values of 250 MPa over the laminate using E-Glass fiber and 261 MPa over the laminate using S-Glass fiber. Maximum von-Mises stress in both the types of laminates was in the range of 370-380 MPa that was close to 372 MPa i.e. the yield strength of aluminum alloy. But the stress was less than 415 MPa i.e. the ultimate tensile strength of aluminum alloy. Critical values of $\sigma_{y,applied}$ were in good agreement with theoretically obtained yield strength values of the laminates. Error of the order of 7.4 % was recorded in both the types of laminates that is acceptable in numerical solutions. Yield strength of laminate with S-Glass fiber was again found to be higher than that using E-Glass fiber.

4.2 Experimental work

Glare laminates with prepregs of E-Glass fibers were fabricated in accordance with the procedure specified in Section 2.1. Aluminum alloy sheets, cold rolled from thickness of 2 mm to 0.4 mm, were re-heat treated to achieve T6 state. Prepregs were prepared and stored in cold environment prior to use. Post laminate fabrication, residual stresses were measured in *y* direction at various arbitrary locations on external aluminum alloy layers of the laminates by X-ray diffraction technique. Following parameters were used in the measurement system:-

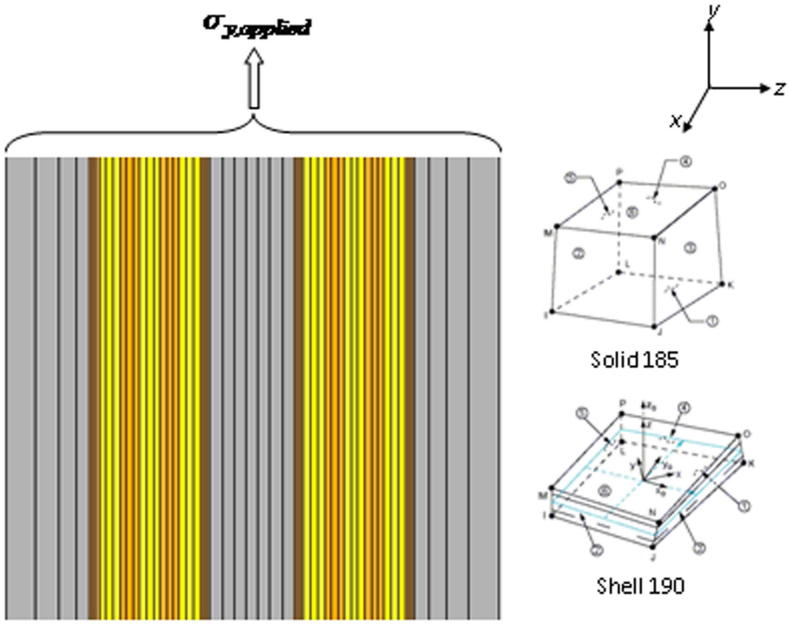

Fig. 3. Mesh model of Glare (Cross sectional view at one end)

Table 2. Magnitude of residual stress in material layers

	x dir. (MPa)	*y* dir.(MPa)
Laminate with E-Glass fiber		
Aluminum, *al*	+ 46.17	+ 48.36
Fiber, *f*	- 173.92	-171.02
Resin, *r*	+ 25.59	+25.73
Laminate with S-Glass fiber		
Aluminum, *al*	+ 44.17	+53.86
Fiber, *f*	- 212.73	-200.16
Resin, *r*	+ 25.50	+25.98
(+ve and –ve denote tensile and compressive stress state respectively)		

i) Radiation: CrKα
ii) 2θ: 139.3 deg.
iii) Spot size: 3 mm
iv) Exp. Time: 15s, 3/3 tilts, -45/45 deg. psi angles
v) Calculation: Cross correlation, linear background
vi) Measurement method: Modified $d(\sin^2\varphi)$

As expected, the residual stresses were mostly found to be tensile in nature due to higher coefficient of thermal expansion of aluminum alloy than that of the laminate. The magnitudes of residual stresses (MPa) were obtained as follows :- +22.2, +36.9, +12.6, -0.5, +9.5 in Test laminate 1 and +14.3,+18.9, +24.9, -0.2, +17.3 in Test laminate 2. Average residual stress was equal to +15.59 MPa (tensile). The value was lower than theoretically estimated value of +48.36 MPa (tensile). The experimental findings also revealed non-uniform residual stress patterns.

Refer Fig. 5. Several Glare laminates were subjected to uni-axial tension in *y* direction, as per the tension test (ASTM D3039), at test speed of 1-2 mm/min [10]. The load was gradually increased until the fibers split upon breaking leading to the fracture of the laminate. Since aluminum alloy and fiber layers did not separate from each other in each laminate during the test, a strong adhesive bond between the layers was confirmed that in turn supported the correctness of adopted volume fractions of fiber and resin in prepregs and the bonding parameters employed to join prepregs with aluminum alloy

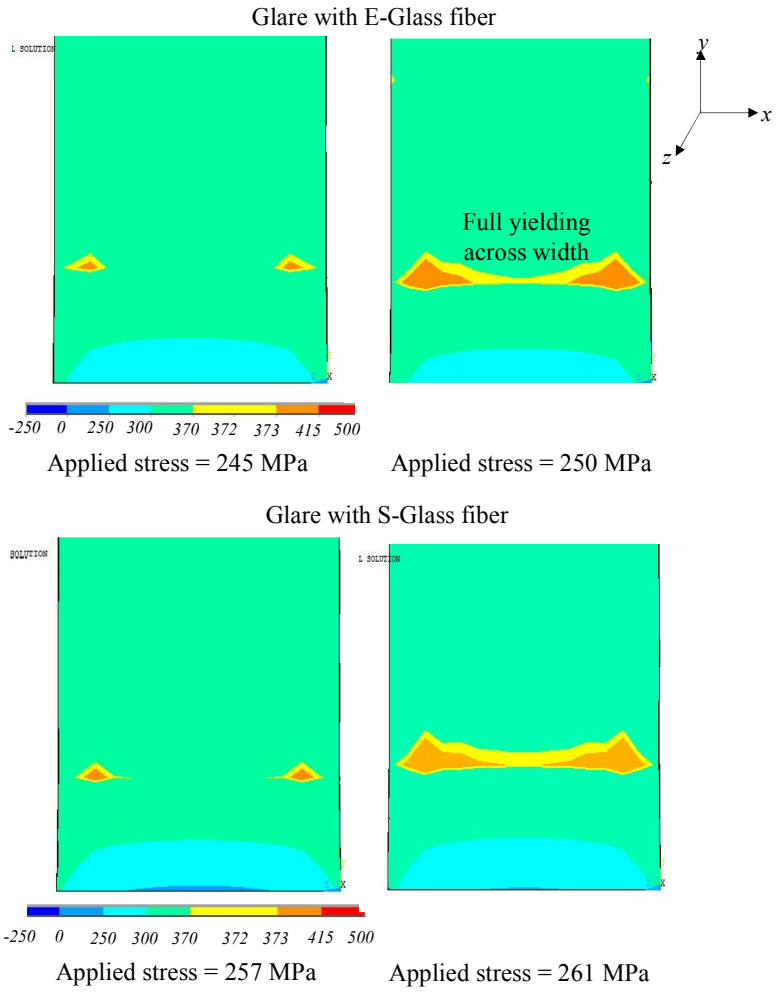

Fig. 4. von-Mises stress plots in aluminum alloy layer of Glare

layers during fabrication of the laminates. Yield load, *P*, at the instant when aluminum alloy layers exhibited signs of yielding, prior to laminate fracture, was recorded from load-extension plot. YS_{Glare} estimated from, $YS_{Glare} = \frac{P}{\text{Laminate width} \times \text{Laminate thickness}\,(\text{Experimental values})}$, for three test laminates were obtained as 273.05, 269.67 and 277.28 (MPa). Average value of YS_{Glare} was found to be 273.33

MPa that was quite close to the theoretical value of 270 MPa. Maximum error of 2.6 % was attributed to the difference in magnitude of experimental and theoretical values of residual

stress in aluminum alloy layers. Lower residual stress necessitated increase in applied tension over test laminates for aluminum alloy layers to yield thereby resulting in higher laminate yield strength in comparison with theoretical result. Reduced yield strength of Glare vis-à-vis aluminum alloy was once again proved.

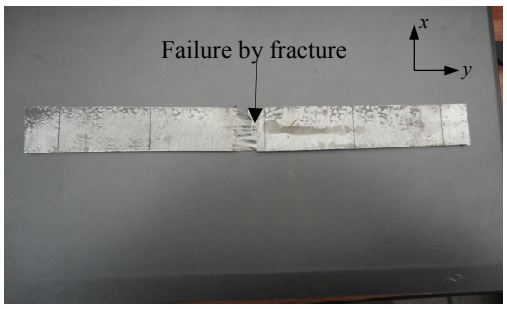

Fig. 5. Tested laminate

5. CONCLUSIONS

A theoretical model for estimation of yield strength of fiber metal laminate is presented. The model is tested over 4A-3/2 Glare laminate that comprises three thin 2014-T6 aerospace aluminum alloy layers alternately bonded adhesively with two prepregs, each prepreg built up of three uni-directional glass fiber layers laid in longitudinal and transverse directions. Laminates made with prepregs of E-Glass and S-Glass fibers are investigated separately under uni-axial tension. The model is validated by finite element analysis and experiments. The following conclusions are drawn based on the results reported in the paper:-

i) Yield strength of Glare is less than that of 2014-T6 aluminum alloy with use of S-Glass fiber resulting in higher laminate yield strength than with the use of E-Glass fiber. Since light weight composite prepregs are employed in the construction of Glare, reduced yield strength of Glare vis-à-vis monolithic aluminum alloy member of identical dimensions as that of the laminate is not expected to result in substantial difference between the specific strengths of the two.

ii) Despite minor variations in patterns and magnitudes of theoretically predicted and experimentally measured residual stresses in aluminum alloy layers of the laminates, the results from finite element analysis and tensile tests conducted over the laminates are in good agreement with theoretical estimations that supports the viability and usefulness of the model.

iii) Since the model is developed from basic principles, it is versatile and is applicable to any type of fiber metal laminate involving different material combinations, varying number and dimensions of material layers.

Appendix A

***A.1** Material stiffness matrices*

Aluminum alloy, $\{M\}_{al} = \begin{bmatrix} 80.79 & 26.66 & 0 \\ 26.66 & 80.79 & 0 \\ 0 & 0 & 27.06 \end{bmatrix}$ GPa

Resin, $\{M\}_{r} = \begin{bmatrix} 3.92 & 1.29 & 0 \\ 1.29 & 3.92 & 0 \\ 0 & 0 & 1.25 \end{bmatrix}$ GPa

E-Glass fiber, $\{M\}_{f0} = \{M\}_{f90} = \begin{bmatrix} 74.61 & 16.41 & 0 \\ 16.41 & 74.61 & 0 \\ 0 & 0 & 29.70 \end{bmatrix}$ GPa

S-Glass fiber, $\{M\}_{f0} = \{M\}_{f90} = \begin{bmatrix} 89.84 & 19.76 & 0 \\ 19.76 & 89.84 & 0 \\ 0 & 0 & 35 \end{bmatrix}$ GPa

A.2 *Laminate stiffness matrices*

With E-Glass fiber

$$\{M\}_{Glare} = \begin{bmatrix} 61.31 & 18.13 & 0 \\ 18.13 & 61.31 & 0 \\ 0 & 0 & 21.72 \end{bmatrix}, \quad \{M\}_{Glare}^{-1} = \begin{bmatrix} 0.0178 & -0.0052 & 0 \\ -0.0052 & 0.0178 & 0 \\ 0 & 0 & 0.046 \end{bmatrix}$$

With S-Glass fiber

$$\{M\}_{Glare} = \begin{bmatrix} 65.09 & 18.95 & 0 \\ 18.95 & 65.09 & 0 \\ 0 & 0 & 23.03 \end{bmatrix}, \quad \{M\}_{Glare}^{-1} = \begin{bmatrix} 0.0167 & -0.00488 & 0 \\ -0.00488 & 0.0167 & 0 \\ 0 & 0 & 0.0434 \end{bmatrix}$$

Appendix B

B.1 *Evaluation of coefficients of thermal expansion of laminate*

Volume of fiber layer $= V_f$

Volume of resin layer $= V_r$

Volume of composite layer (fiber + resin), $V_c = V_{c0} = V_{c90} = V_f + V_r$

Volume of aluminum layer $= V_{al}$

Volume fraction of fiber in composite layer, $v'_f = \dfrac{V_f}{V_f + V_r}$

Volume fraction of resin in composite layer, $v'_r = \dfrac{V_r}{V_f + V_r} = 1 - v'_f$

Volume fraction of aluminum in laminate, $v'_{al} = \dfrac{3V_{al}}{3V_{al} + 6V_c}$

Volume fraction of composite *c*0 in laminate, $v'_{c0} = \dfrac{4V_{c0}}{4V_{c0} + 2V_{c90} + 3V_{al}}$

Volume fraction of composite *c*90 in laminate, $v'_{c90} = \dfrac{2V_{c90}}{4V_{c0} + 2V_{c90} + 3V_{al}}$

Longitudinal modulus of elasticity of composite (along fiber), $E_{lc} = E_f v'_f + E_r v'_r$

Transverse modulus of elasticity of composite (perpendicular to fiber), $E_{tc} = \frac{E_f E_r}{v'_f E_r + v'_r E_f}$

Major poisson's ratio of composite (along fiber w.r.t. perpendicular to fiber), $\upsilon_{majc} = v'_f \upsilon_f + v'_r \upsilon_r$

Minor poisson's ratio of composite (perpendicular to fiber w.r.t. along fiber), $\upsilon_{minc} = \upsilon_{majc} \frac{E_{tc}}{E_{lc}}$

Longitudinal coeff. of thermal expansion of composite (along fiber), $\alpha_{lc} = \frac{E_f v'_f \alpha_f + E_r v'_r \alpha_r}{E_f v'_f + E_r v'_r}$

Transverse coeff. of thermal expansion of composite (perpendicular to fiber)

$\alpha_{tc} = \alpha_f v'_f (1+\upsilon_f) + \alpha_r v'_r (1+\upsilon_r) - \upsilon_{majc} \alpha_{lc}$

Major poisson's ratio of laminate (y w.r.t. x), $\upsilon_{majlam} = \upsilon_{majc} v'_{c0} + \upsilon_{al} v'_{al} + \upsilon_{minc} v'_{c90}$

Longitudinal coeff. of thermal expansion of laminate (y dir.)

$\alpha_{ylam} = \frac{E_{lc} v'_{c0} \alpha_{lc} + E_{tc} v'_{c90} \alpha_{tc} + E_{al} v'_{al} \alpha_{al}}{E_{lc} v'_{co} + E_{tc} v'_{c90} + E_{al} v'_{al}}$

Transverse coeff. of thermal expansion of laminate (x dir.)

$\alpha_{xlam} = \alpha_{lc} v'_{c0} (1+\upsilon_{majc}) + \alpha_{al} v'_{al} (1+\upsilon_{al}) + \alpha_{tc} v'_{c90} (1+\upsilon_{minc}) - \upsilon_{majlam}\, \alpha_{ylam}$

Acknowledgment
Research was funded by the Science and Engineering Research Council, Department of Science and Technology, India vide Grant No. SR/S3/MERC/042/2009.

References

[1] G. Lawcock, L.Ye, Y.W. Mai and C.T. Sun, "The effect of adhesive bonding between aluminum and composite prepreg on the mechanical properties of carbon-fiber-reinforced metal laminates," Composites Science and Technology, vol. 57, pp.35-45, 1997.

[2] M. Kawai, M. Morishita, S. Tomura and K. Takumida, "Inelastic behavior and strength of fiber-metal hybrid composite: Glare," International Journal of Mechanical Sciences, vol. 40, pp.183-198, 1998.

[3] P. Cortes and W.J. Cantwell, "The tensile and fatigue properties of carbon fiber-reinforced PEEK-titanium fiber-metal laminates," Journal of Reinforced Plastics and Composites, vol. 23, pp.1615-1623, 2004.

[4] S.M.R. Khalili, R.K. Mittal and S.G. Kalibar, "A study of the mechanical properties of steel/aluminum/GRP laminates," Materials Science and Engineering A, vol. 412, pp.137-140, 2005.

[5] S.E.M. Torshizi, S. Dariushi, M. Sadighi and P. Safarpour, "A study on tensile properties of a novel fiber/metal laminate." Materials Science and Engineering A, vol. 527, pp. 4920-4925, 2010.

[6] T. Sinmazcelik, E. Avcu, M.O. Bora and O. Coban, " A review: fiber metal laminates, background, bonding types and applied test methods," Materials and Design, vol. 32, pp. 3671-3685, 2011.

[7] R.G.J. Van Rooijen, J. Sinke, T.J. De Vries and S. Van Der Zwaag, " The bearing strength of fiber metal laminates," Journal of Composite Materials, vol. 40, pp. 5-19, 2006.

[8] P.P. Krimbalis, C. Poon, Z. Fawaz and K. Behdinan, "Prediction of bearing strength in fiber metal laminates," Journal of Composite Materials, vol.41, pp.1137-1157, 2007.

[9] H. Schuerch, "Prediction of compressive strength in uniaxial boron fiber-metal matrix composite materials," AIAA Journal, vol. 4, pp. 102-106, 1996.

[10] S. Bhat and S. Narayanan, "On fabrication and testing of Glare," Journal of Engineering and Applied Sciences, vol.9, p.1610, 2014.

Sunil Bhat, Ph.D., Worked on various projects, Published papers in national and international journals and conference proceedings.

Suresh Nagesh, Ph.D., Worked on various projects, Published papers in national and international journals and conference proceedings.

C.K. Umesh, M.E., Working as Assistant Professor.

S. Narayanan, Ph.D., Worked on various projects, Published papers in national and international journals and conference proceedings.